Water availability limits tree productivity, carbon stocks, and carbon residence time in mature forests across the western United States

Logan T. Berner *[1], Beverly E. Law [1], and Tara W. Hudiburg [2]

[1] Department of Forest Ecosystems and Society
Oregon State University
321 Richardson Hall
Corvallis, Oregon 97331-2212

[2] Department of Forest, Rangeland, and Fire Sciences
University of Idaho
875 Perimeter Drive
Moscow, Idaho 83844-1133

* Corresponding Author:
logan.berner@oregonstate.edu
phone: 702-683-9987
fax: 541-737-5814

Running header:
Water limitations on forests in the western US

Keywords:
Bioclimatic gradient, carbon cycle, climate change, climate moisture index, forest inventory, MODIS, satellite remote sensing, biomass

Type of paper:
Primary research article

Abstract

Water availability constrains the structure and function of terrestrial ecosystems and is projected to change in many parts of the world over the coming century. We quantified the response of tree net primary productivity (NPP), live biomass (BIO), and mean carbon residence time (CRT=BIO/NPP) to spatial variation in water availability in the western US. We used forest inventory measurements from 1,953 mature stands (>100 years) in Washington, Oregon, and California (WAORCA) along with satellite and climate data sets covering the western US. We summarized forest structure and function in both domains along a 400 cm yr^{-1} hydrologic gradient, quantified with a climate moisture index (CMI) based on the difference between precipitation and reference evapotranspiration summed over the water-year (October-September) and then averaged annually from 1985-2014 ($CMI_{\overline{wy}}$). Median NPP, BIO, and CRT computed at 10 cm yr^{-1} intervals along the $CMI_{\overline{wy}}$ gradient increased monotonically with increasing $CMI_{\overline{wy}}$ across both WAORCA (r_s=0.93-0.96, p<0.001) and the western US (r_s=0.93-0.99, p<0.001). Field measurements from WAORCA showed that median NPP increased from 2.2 to 5.6 Mg C ha^{-1} yr^{-1} between the driest and wettest 5% of sites, while BIO increased from 26 to 281 Mg C ha^{-1} and CRT increased from 11 to 49 years. The satellite data sets revealed similar changes over the western US, though these data sets tended to plateau in the wettest areas, suggesting that additional efforts are needed to better quantify NPP and BIO from satellites in high-productivity, high-biomass forests. Our results illustrate that long-term average water availability is a key environmental constraint on tree productivity, carbon storage, and carbon residence time in mature forests across the western US, underscoring the need to assess potential ecosystem response to projected warming and drying over the coming century.

1 Introduction

Water availability strongly constrains the distribution of plants on Earth's land surface (Holdridge, 1947; Major, 1963) and the resulting structure and function of terrestrial ecosystems (Churkina and Running, 1998; Law et al., 2002; Schuur, 2003). For instance, desert (Whittaker and Niering, 1975), grassland (Yang et al., 2008) and forest productivity (Law et al., 2002; Schuur, 2003; Berner and Law, 2015) differ widely among sites with contrasting water availability. Water availability is shaped by regional climate (e.g., precipitation, atmospheric evaporative demand), as well as by local topography and soils (Webb et al., 1983). Water availability is projected to change in many parts of the world over the coming century in response to continued atmospheric warming from sustained anthropogenic greenhouse gas emissions (Collins et al., 2013; Dai, 2013; Walsh et al., 2014). Societies depend on the goods and services provided by terrestrial ecosystems (e.g., forests; Williams, 2006) and thus it is imperative to elucidate climatic controls over ecosystem structure and function to help anticipate and mitigate potential impacts of ongoing climatic change.

The western United States is a region where pronounced spatial variation in water availability exerts a strong influence over forest structure and function. For instance, average annual precipitation varies over 500 cm yr^{-1} across this region, with particularly steep hydrologic gradients in the Pacific Northwest (Daly et al., 2008). Differences in water availability gives rise to forest communities that range from dry, low-productivity woodlands to high-productivity coastal temperate rainforests where live tree biomass (BIO) attains levels thought to be exceeded only by primary *Eucalyptus regnans* forests in southern Australia (Waring and Franklin, 1979; Keith et al., 2009).

Prior studies drew on small networks of field sites (n < 20) to investigate how tree net primary productivity (NPP) and BIO varied among mature stands spread along hydrologic gradients in parts of this region (Whittaker and Niering, 1975; Gholz, 1982; Webb et al., 1983; Berner and Law, 2015). Tree BIO and NPP can vary widely with stand age (Hudiburg et al., 2009) and thus these studies focused on mature stands (stand age generally > 100 years) where BIO and NPP had somewhat stabilized after reaching their 'climatic potential.' These studies showed that BIO and NPP tended to increase linearly or curvilinearly across sites as average water availability increased (Whittaker and Niering, 1975; Gholz, 1982; Webb et al., 1983; Berner and Law, 2015). These spatial relationships are thought to reflect long-term climatic constraints on ecosystem structure (e.g., BIO) and function (e.g., NPP) that are shaped by gradual shifts in community composition and population size (Jin and Goulden, 2014). The field studies mentioned above make a compelling case that water availability is an important determinant of BIO and NPP in mature stands, yet these studies were based on a small number of field sites selected using a set of criteria (e.g., mature stands near a road) rather than on a large sample of mature stands in the region.

Several of these earlier field studies also indicated that plant communities accumulated more BIO per unit of NPP in progressively wetter areas, suggesting slower turnover of plant BIO as climate became wetter (Whittaker and Niering, 1975; Webb et al., 1983). Mean carbon residence time (CRT) describes the average duration that a carbon molecule will remain in a specific pool (Waring and Running, 2007) and for CRT in live biomass can be computed as BIO/NPP assuming that BIO remains constant over time (Whittaker, 1961; Friend et al., 2014). Carbon residence time in live biomass is also known as the *biomass accumulation ratio* (Whittaker, 1961) and ranged, for instance, from ~2 years in a hot desert shrubland to ~75 years

in an wet, old-growth Douglas-fir forest (Webb et al., 1983). Differences in CRT among plant communities with contrasting climate are potentially associated with shifts in carbon allocation (e.g. short-lived fine roots and foliage vs. long-lived stem wood) and disturbance regimes (Girardin et al., 2010). Together, these field studies illustrate that forest structure and function are constrained by water availability in parts of the western US; however, additional efforts are needed to assess these relationships at larger scales across the region, particularly given that climate models project a pronounced shift towards hotter, drier conditions over much of the region during the coming century (Collins et al., 2013; Walsh et al., 2014; Cook et al., 2015).

Our objective in this study was to explore how forest structure and function change along spatial gradients in water availability across the western US. We used the average water-year climate moisture index ($CMI_{\overline{wy}}$; 1985-2014) as an indicator of long-term water availability (Webb et al., 1983; Hogg and Hurdle, 1995), which we computed as the cumulative difference between precipitation (P) and reference evapotranspiration (ET_0) over the approximate seasonal cycle of soil water recharge and draw-down (October-September). Furthermore, we focused on forest stands that were at least 100 years old because field surveys from the region indicated that BIO and NPP reached much of their 'climatic potential' after a century, yet we acknowledge that BIO tends to gradually increase and NPP remains stable or gradually declines during subsequent centuries (Hudiburg et al., 2009). Building on prior field studies (e.g., Gholz, 1982; Webb et al., 1983; Berner and Law, 2015), we hypothesized that long-term water availability limits tree NPP, BIO, and CRT in mature forest stands across the region. We thus predicted that tree NPP, BIO, and CRT in mature forests would increase with increasing $CMI_{\overline{wy}}$. Tree NPP, BIO, and CRT were based on above- and below-ground components. We tested these hypotheses first across Washington, Oregon, and California (WAORCA) using forest inventory measurements from

1,953 sites and then across 18 Mha of mature forest in the western US using satellite remote sensing data sets. These data sets included three national biomass maps, along with NPP derived from the Moderate Resolution Imaging Spectroradiometer (MODIS). Forest inventories provide rigorous, though spatially-limited field measurements of forest structure and function, while satellite remote sensing provides spatially-continuous, albeit modeled estimates of forest structure and function across large domains.

2 Materials and methods

2.1 Data sets and preprocessing

2.1.1 Field estimates of tree biomass, productivity, and carbon residence time

We used field measurements to estimate tree BIO (BIO_{field}; Mg C ha^{-1}), NPP (NPP_{field}; Mg C ha^{-1} yr^{-1}), and CRT (CRT_{field}; year) at 1,953 forest inventory sites located in mature stands spread across WAORCA. These 1-ha sites were surveyed by the US Forest Service Forest Inventory and Analysis (FIA) program between 2001 to 2006 and comprise a representative sample of forest lands (tree cover > 10%) in the region (Bechtold and Patterson, 2005). The inventory sites occurred at elevations ranging from 5 m to 3,504 m, with an average (±1SD) elevation of 1429±677 m. We included sites in our analysis when stand age was at least 100 years. Stand age was defined as the average age of the oldest 10% of trees, where individual tree age was determined on survey plots using increment cores (Van Tuyl et al., 2005). Tree BIO_{field} and NPP_{field} were computed for each site as part of a prior study (Hudiburg et al., 2011). Tree BIO_{field} was estimated using regional allometric equations for tree components (e.g., stem, branch, bark,

143 foliage, and coarse roots) based on tree diameter and/or height (Means et al., 1994; Law et al.,
144 2001), along with estimates of fine root mass derived from a relationship with leaf area index
145 (LAI; m^2 leaf m^{-2} ground; Van Tuyl et al. 2005). Tree NPP_{field} was estimated based on changes in
146 above- and below-ground woody biomass over a 10-year interval plus annual foliage and fine
147 root turn-over. See Hudiburg et al. (2011) for additional details. We then computed CRT_{field} in
148 live tree biomass as the ratio of BIO_{field} to NPP_{field}.

149

150 **2.1.2 Remote sensing estimates of tree biomass, productivity, and carbon residence time**

151 We used satellite remote sensing and ancillary data sets to estimate BIO (BIO_{sat}), NPP (NPP_{sat}),
152 and CRT (CRT_{sat}) across mature forests in the western US. BIO_{sat} included the same component
153 carbon pools as BIO_{field} (i.e, stem, branch, bark, foliage, coarse roots and fine roots). We
154 quantified the amount of carbon in stems, branches, and bark using an ensemble of three
155 satellite-derived data sets that depicted live tree aboveground biomass (AGB; excluded foliage)
156 circa 2000 to 2008 (Blackard et al., 2008; Kellndorfer et al., 2012; Wilson et al., 2013). Each
157 map was generated using satellite and geophysical (e.g., climate, topography) data sets to
158 spatially extrapolate forest inventory measurements over the conterminous US. We acquired
159 these maps at 250-m spatial resolution and then converted two of the maps (Blackard et al.,
160 2008; Kellndorfer et al., 2012) from dry biomass to carbon assuming a 50% conversion factor
161 (Smith et al., 2006). We then reprojected these maps onto a uniform grid in an equal area
162 projection, masked them to the common forest extent, and then averaged the AGB for each pixel
163 across the three biomass maps. We used the biomass map ensemble average in the subsequent

164 analysis, recognizing that pixel-wise estimates of AGC can vary notably among individual maps
165 (Neeti and Kennedy, 2016).

166 After deriving spatial estimates of carbon storage in AGB, we then estimated carbon
167 storage in coarse roots, fine roots, and foliage for each 250-m forested pixel. As with AGB, we
168 assumed that roots and foliage were 50% carbon (Smith et al., 2006; Berner and Law, 2016). We
169 computed coarse root biomass based on an empirical relationship with AGB (Cairns et al., 1997)
170 and fine root biomass based on an empirical relationship with peak summer LAI (Van Tuyl et al.,
171 2005). Spatial estimates of LAI were available globally at 1-km resolution from NASA's
172 Moderate Resolution Imaging Spectroradiometer (MODIS) as part of the MOD15A2 (Collection
173 5) data set (Myneni et al., 2002). We obtained these LAI estimates at 8-day intervals during July
174 and August (late-summer) from 2000 to 2014 for the western US. We then (1) excluded poor-
175 quality pixels using the quality control flags; (2) computed average late-summer LAI over the
176 15-year period; and (3) reprojected and resampled the data set to the common 250-m resolution
177 equal area grid. We used average late-summer MODIS LAI to computed both fine root biomass
178 (as described above) and foliage biomass. Foliage biomass was estimated for each pixel by
179 dividing LAI by the average specific leaf area (SLA; g C m^{-2} leaf) of the forest type found in that
180 pixel. We aggregated an existing map of forest type (Ruefenacht et al., 2008) into nine classes
181 (e.g., *Pinus ponderosa,* true fir) and then varied SLA among classes using species-, genus-, or
182 division-specific estimates of average SLA from a recent leaf trait synthesis (Berner and Law,
183 2016). We then estimated BIO_{sat} for each 250-m resolution pixel by summing the above- and
184 below-ground carbon pools.

185 We quantified regional NPP using the satellite-derived MODIS primary productivity data
186 set (NPP_{sat}; MOD17A3 v. 55). The MODIS light-use efficiency model predicts annual NPP at 1-

187 km resolution across global terrestrial ecosystems by incorporating estimates of absorbed
188 photosynthetically active radiation (APAR), LAI, and land cover derived from MODIS together
189 with plant physiological characteristics and climate data (Running et al., 2004; Zhao et al.,
190 2010). The model first predicts daily gross primary productivity (GPP) based APAR and the
191 efficiency with which APAR is converted to biomass (ε), which is affected by low temperatures
192 (frost) and high vapor pressure deficit (VPD) inducing stomatal closure. The model then
193 estimates plant respiration (R) at daily to annual increments and subsequently computes annual
194 NPP as the cumulative difference between GPP and R. These estimates thus reflect NPP
195 allocated both above- and below-ground. We acknowledge a degree of circularity in relating
196 NPP_{sat} to CMI given that both computations incorporate temperature data, specifically,
197 temperature-effects on VPD. We obtained annual NPP estimates from 2000 to 2014 for the
198 western US, reprojected the data onto an equal area grid, and then averaged over years.

199 Several additional preprocessing steps were required after deriving forest BIO_{sat} and
200 NPP_{sat}. These included masking both BIO_{sat} and NPP_{sat} to areas mapped as forest by the MODIS
201 land cover map (Friedl et al., 2010) and then further masking these data sets to include only areas
202 where stand age was at least 100 years. The map of stand age reflected conditions c. 2006 and
203 was produced by Pan et al. (2011) by combining forest inventory measurements, information on
204 historical fires, and optical satellite imagery. We applied these 1-km resolution masks to the 250-
205 m resolution BIO_{sat} assuming homogenous land cover and stand age within each 1-km pixel. We
206 then aggregated BIO_{sat} from 250-m to 1-km resolution and computed CRT_{sat} as the ratio of
207 BIO_{sat} to NPP_{sat}.

208

2.1.3 Climate data sets and derivation of the climate moisture index

We quantified water availability using a climate moisture index (CMI) that was computed at monthly time steps as precipitation minus ET_0 (Webb et al., 1983; Hogg, 1994). We summed monthly CMI over each water-year (October in year *t-1* to September in year *t*) from 1985 to 2014 and then averaged over years to produce a 30-year climatology ($\overline{CMI_{wy}}$; cm yr^{-1}). The water year represents the approximate annual cycle of soil water recharge and withdrawal (Thomas et al., 2009). We obtained estimates of monthly precipitation from the Parameter-elevation Relationships on Independent Slopes Model (PRISM; Daly et al., 2008), which interpolated weather station measurements onto a 4-km resolution grid. We then estimated monthly ET_0 using the Food and Agricultural Organizations (FAO) Penman-Monteith equation (FAO-56; Allen et al., 1998), where

$$ET_0 = \frac{0.408\Delta\,(R_n - G) + \gamma\left(\frac{900}{T+273}\right)U(e_s - e_a)}{\Delta + \gamma\,(1 + 0.34\,U)}$$

Variables included net incoming radiation (R_n), soil heat flux (G), mean daily temperature (T), wind speed (U), and both saturation (e_s) and actual vapor pressure (e_a), as well as the psychrometric constant (γ) and the slope of the vapor pressure curve (Δ). We quantified R_n and U using monthly climatologies from the North American Land Data Assimilation System-2 (NALDAS-2; ~12-km resolution) that were based on measurements from 1980-2009 (Mitchell et al., 2004). We derived G, T, e_s, and e_a from PRISM temperature data following Zotarelli et al. (2010). We also computed $\overline{CMI_{wy}}$ based on ET_0 derived using the modified-Hargreaves approach (Hargreaves and Samani, 1985; Droogers and Allen, 2002) and found that our analysis was robust to differences in methods used to compute ET_0 (results not shown). After computing

230 $CMI_{\overline{wy}}$, we then resampled these data using the nearest neighbor approach to match the
231 footprints of both the 1-km NPP and 250-m BIO remote sensing data sets.

232

233 **2.2 Analysis**

234 We quantified the response of tree NPP, BIO, and CRT to changes in $CMI_{\overline{wy}}$ across both
235 WAORCA and the broader western US. We specifically focused on areas where $CMI_{\overline{wy}}$ was
236 between -200 and 200 cm yr^{-1}, conditions which occurred both in WAORCA and in the broader
237 region. This range encompassed 98% of forest area in the western US; the paucity of data in the
238 remaining 2% of forest area that was either drier or wetter precluded rigorous analysis. We
239 divided the landscape along this gradient into 10 cm yr^{-1} non-overlapping bins and then
240 summarized forest characteristics in each bin by computing the median, along with the 10^{th}, 25^{th},
241 75^{th} and 90^{th} percentiles. Forest characteristics were summarized separately for the field and
242 remote sensing data sets. There were a minimum of 10 and a maximum of 114 field sites in each
243 bin. We then assessed the association between the median forest characteristic (i.e., NPP, BIO,
244 and CRT) in each bin and $CMI_{\overline{wy}}$ across the bioclimatic gradient using nonparametric
245 Spearman's rank correlation. This test yields a coefficient (r_s) between -1 and +1, where a value
246 of +1 indicates a perfect monotonically increasing relationship, a value of zero indicates no
247 covariation between the two variables, and a value of -1 indicates a perfect monotonically
248 decreasing relationship. The test is analogous to Pearson's correlation where the data have first
249 been ranked. We assessed the association between forest characteristics and $CMI_{\overline{wy}}$ using
250 Spearman's correlation rather than nonlinear regression because our intent was to describe the
251 general relationship rather than develop a predictive model. We performed data preprocessing,

252 analysis, and visualization using ArcGIS 10 (ESRI, Redlands, CA) and *R* statistical software (R
253 Core Team, 2015), relying extensively on the *R* packages *raster* (Hijmans and van Etten, 2013)
254 and *dplyr* (Wickham and Francois, 2015).
255

256 ## 3 Results

257 Average annual water availability varied widely across both WAORCA and the broader western
258 US from 1985-2014 (Fig. 1a, b). The $CMI_{\overline{wy}}$ ranged from a minimum of -330 cm yr^{-1} in southern
259 California and Arizona to a maximum of 490 cm yr^{-1} in the Olympic Mountains in northwestern
260 Washington. Forests mapped by MODIS occurred in areas where $CMI_{\overline{wy}}$ was between -340 and
261 490 cm yr^{-1}, though 98% of forest area occurred between -200 and 200 cm y^{-1}, and 72% occurred
262 between -100 and 100 cm yr^{-1}. Average (±1 SD) $CMI_{\overline{wy}}$ in forested areas was -40±80 cm yr^{-1}.
263 The Coast Range and Cascade Mountains in Washington and Oregon were the wettest areas,
264 with $CMI_{\overline{wy}}$ generally >100 cm yr^{-1}. Water availability decreased rapidly in the rain shadows east
265 of the Cascades and Sierra Nevada, giving rise to very steep $CMI_{\overline{wy}}$ gradients. For instance,
266 annual $CMI_{\overline{wy}}$ in northern Oregon decreased nearly 350 cm over ~30 km between high-elevation
267 forests in the Cascades and low-elevation woodlands in the eastern foothills of the Cascades. The
268 range in $CMI_{\overline{wy}}$ encountered along this gradient in the Cascades almost spanned the full range in
269 $CMI_{\overline{wy}}$ that supported 98% of forest area in the western US. Dry forests occurred along the low-
270 elevation margins of mountain ranges throughout continental areas, though the largest tract of
271 dry forest was found in Arizona and New Mexico.

Tree NPP, BIO, and CRT varied substantially across both WAORCA and the broader western US in response to variation in $CMI_{\overline{wy}}$ (Fig. 1, 2, Table 2). We focused on forests in areas where $CMI_{\overline{wy}}$ was between -200 and 200 cm yr^{-1} given the paucity of land and measurements in the 2% of forest area that was either drier or wetter. Median NPP_{field}, BIO_{field}, and CRT_{field} all exhibited a strong, positive association with $CMI_{\overline{wy}}$ (r_s=0.93-0.96, p<0.001). Median NPP_{field} increased 155% between the driest and wettest 5% of sites in WAORCA (Fig. 2a), while median BIO_{field} and CRT_{field} increased 997% and 358%, respectively, between these sites (Fig. 2b, c; Table 2). The relationship in each case was slightly curvilinear. There were also strong, positive relationships among median NPP_{field}, BIO_{field}, and CRT_{field} along the WAORCA bioclimatic gradient (r_s=0.90-0.96, p<0.001).

Broadly similar patterns were evident when tree NPP_{sat}, BIO_{sat}, and CRT_{sat} were examined across the western US using remote sensing data sets (Fig. 1b, c, d, 2c, d; Table 2). Median NPP_{sat}, BIO_{sat}, and CRT_{sat} all showed a strong, positive relationship with $CMI_{\overline{wy}}$ (r_s=0.93-0.99; p<0.001). Median NPP_{sat} increased 97% between the driest and wettest 5% of forested areas along the regional $CMI_{\overline{wy}}$ gradient (Fig. 2d, Table 2). Similarly, median BIO_{sat} and CRT_{sat} increased 410% and 160%, respectively, between the driest and wettest areas (Fig. 2e, f, Table 2). The response of median NPP_{sat}, BIO_{sat}, and CRT_{sat} to increased $CMI_{\overline{wy}}$ was more curvilinear than the field measurements and plateaued in areas where $CMI_{\overline{wy}}$ exceeded ~100 cm yr^{-1}. Furthermore, while magnitude of NPP_{sat} and NPP_{field} response to $CMI_{\overline{wy}}$ were similar, the magnitude of BIO_{sat} and CRT_{sat} responses to increased $CMI_{\overline{wy}}$ were much more muted than the magnitude of response in BIO_{field} and CRT_{field}. Nevertheless, field- and satellite-derived estimates of median NPP, BIO, and CRT were strongly correlated (r_s=0.90-0.95; p<0.001).

294 Furthermore, there were again strong relationships among median NPP_{sat}, BIO_{sat}, and CRT_{sat}
295 along the western US bioclimatic gradient (r_s=0.93-0.97, p<0.001).

296

297 # 4 Discussion and conclusions

298 ## 4.1 Climate moisture index

299 Water availability exerted a strong influence on tree NPP, BIO, and CRT among mature forests
300 in the western US. We chose to quantify water availability using an index that accounted for both
301 precipitation and energy-mediated ET_0, recognizing that both of these factors contribute to the
302 relative water stress experienced by plants within an ecosystem (Webb et al., 1983). We
303 acknowledge that this index has several short-comings. For instance, the index does not account
304 for spatial variation in soil water storage capacity, which can be crucial for determining plant
305 performance during drought (Peterman et al., 2013). This might explain some of the variation in
306 NPP and BIO among areas with similar $CMI_{\overline{wy}}$; however, quantifying soil water storage capacity
307 even at individual sites is challenging given uncertainty in soil structure and plant rooting
308 capacity (Running, 1994). The index also does not account for water added via fog drip, which
309 has been shown to supply 13-45% of the water transpired by redwood forests (*S. sempervirens*)
310 (Dawson, 1998) and sustain other forest ecosystems along the California coast (Johnstone and
311 Dawson, 2010; Fischer et al., 2016). This potentially explains why there were areas with low
312 $CMI_{\overline{wy}}$ along the central and northern coast of California that supported forests with higher NPP
313 and BIO than other forests with similar $CMI_{\overline{wy}}$. Furthermore, the index does not account for
314 spatial variation in runoff and thus likely overestimates water availability in the wettest areas

since the fraction of water lost as run-off increases with precipitation (Sanford and Selnick, 2013). Despite its relative simplicity, prior studies showed that CMI was a useful index for explaining interannual variability in fire activity in the southwest US (Williams et al., 2014), as well as forest productivity in northern Siberia (Berner et al., 2013), southern Canada (Hogg et al., 2002), and central Oregon (Berner and Law, 2015). Several studies also found that the index, or its inverse (i.e. ET_0 - P), explained substantial spatial variability in mature forest gross photosynthesis (Law et al., 2002), productivity and biomass across a range of ecosystems (Webb et al., 1983; Hogg et al., 2008; Berner and Law, 2015). Our current study further demonstrates that CMI is a useful, empirical index for assessing climatic constraints on forest ecosystems at large spatial scales.

4.2 Tree net primary productivity

Median tree NPP in mature stands approximately doubled between the driest and wettest areas in both WAORCA and the western US, though in both cases the rate at which NPP increased with $CMI_{\overline{wy}}$ slowed in the wettest areas. Prior field studies conducted at a limited number of field sites in the western US over the past four decades have similarly documented increased tree NPP along spatial gradients of increasing water availability (Whittaker and Niering, 1975; Gholz, 1982; Webb et al., 1983; Berner and Law, 2015). Building on these prior efforts, our current study demonstrates a robust relationship between tree NPP and water availability in mature forests using field measurements from nearly 2,000 inventory plots along with satellite remote sensing estimates of NPP covering ~18 Mha of forestland.

The NPP-$\overline{CMI}_{wy}$ relationship was similar when NPP was assessed using field measurements from across WAORCA or using MODIS covering the western US. The NPP estimates derived from MODIS did level off in the wettest parts of WAORCA ($\overline{CMI}_{wy}$ ≈ 100-200 cm yr^{-1}), whereas this was less evident in the field measurements. The inventory sites and MODIS forestland occurred at similar elevations along the $\overline{CMI}_{wy}$ gradient in WAORCA, suggesting that this discrepancy in NPP was not due to MODIS systematically including cold, high-elevation areas not sampled by the inventory sites. One possibility is that MODIS NPP did not increase in the wettest areas because MODIS becomes less sensitive to increases in the fraction of photosynthetically-active radiation (FPAR) absorbed by plant canopies in densely vegetated areas (Yan et al., 2016). A recent MODIS analysis similarly found that the amount of photosynthetically-active radiation absorbed by plant canopies (APAR = FPAR x PAR) increased asymptotically with increasing mean annual precipitation across plant communities in California (Jin and Goulden, 2014). Forests had higher APAR than other plant communities and, furthermore, exhibited the smallest increase in APAR per unit increase in precipitation of any plant community, suggesting that forest productivity was less sensitive to changes in precipitation than productivity of other plant communities (Jin and Goulden, 2014). In contrast with the field measurements, the asymptotic response of MODIS NPP and APAR to increasing water availability in wet areas suggests that climate impact assessments based on MODIS could underestimate the sensitivity of plant productivity to changes in water availability in wet areas with high biomass.

Mechanistically, the strong NPP-$\overline{CMI}_{wy}$ association reflects the coupling between carbon and water cycling at leaf (Ball et al., 1987) to ecosystem scales (Law et al., 2002). Tree NPP depends on regionally-specific relations with leaf area (Schroeder et al., 1982; Waring, 1983),

359 which largely determine the proportion of incoming solar radiation that is absorbed and thus
360 potentially available to fuel photosynthesis (Runyon et al., 1994). Leaf photosynthesis inevitably
361 leads to transpiration water loss (Ball et al., 1987) that must be balanced against water uptake
362 from the soil so as to prevent the formation of excessive tension on the internal water column
363 that could result in hydraulic failure (Williams et al., 1996; Ruehr et al., 2014). As soil water
364 availability increases, trees are able to support greater leaf area while maintaining water column
365 tensions within physiologically operable ranges, which consequently leads to more
366 photosynthate available to fuel NPP unless trees are limited by other resources (e.g., nitrogen).
367 The decreasing rate at which NPP increased with $\mathrm{CMI}_{\overline{\mathrm{wy}}}$ in the wettest areas is likely due to low
368 temperatures constraining productivity at high-elevations (Runyon et al., 1994; Nakawatase and
369 Peterson, 2006) and heavy cloud-cover limiting solar radiation and thus photosynthesis in coastal
370 areas (Zhao et al., 2010; Carroll et al., 2014). Tree NPP is affected by many biotic (e.g., age) and
371 abiotic factors (e.g., nutrients), yet water availability emerges as a key environmental constraint
372 in the western US.

373

374 **4.3 Tree carbon stocks**

375 Tree BIO increased notably with increasing $\mathrm{CMI}_{\overline{\mathrm{wy}}}$ in mature forests across both WAORCA and
376 the broader western US, reflecting underlying shifts in NPP and, likely, BIO mortality rates due
377 to natural disturbance. Tree biomass is determined by the rates at which carbon is gained via
378 NPP and lost due to tissue senescence and mortality integrated over annual to centennial time
379 scales (Olson, 1963). Hence, the increase in NPP with increasing $\mathrm{CMI}_{\overline{\mathrm{wy}}}$ explains some of the
380 concomitant increase in BIO. Our analysis did not investigate how tissue senescence or mortality

varied along the regional bioclimatic gradient, though a recent study found that BIO mortality rates due to bark beetles and fires were very low in the wettest parts of the western US (e.g., Coast Range and Cascades), while considerably higher in most drier areas (Hicke et al., 2013). Furthermore, the field and satellite data sets also incidentally revealed there was an increase in the median age of stands over 100 years as conditions became wetter, with median stand age ~140 years in the driest areas and 200-240 years in the wettest areas. The general increase in BIO with increasing water availability is thus likely due to higher rates of productivity and potentially lower BIO mortality rates from natural disturbance.

The observed increase in BIO with increasing water availability was generally consistent with prior field studies from this region, yet our study demonstrates this response over a much broader bioclimatic gradient. For instance, early work by Whittaker and Niering (1975) showed that BIO in mature forests tended to increase with a moisture index inferred from community composition along an elevational gradient in Arizona's Santa Catalina Mountains. Subsequent studies focused on five LTER sites spread across the conterminous US (Webb et al., 1983) and at 8-12 sites in Oregon (Gholz, 1982; Berner and Law, 2015) similarly showed a general increase in tree biomass with increasing water availability. Our study included sites that ranged from dry woodlands with little BIO to temperate rainforests with BIO exceeded in few other regions (e.g. max BIO ≈ 950 Mg C ha^{-1}). Tree biomass in our study area has been reported to reach over 2,000 Mg C ha^{-1} in old-growth coastal redwood stands in northern California (Waring and Franklin, 1979), which is thought to be exceeded only by the >3,000 Mg C ha^{-1} attained by old-growth *Eucalyptus regnans* stands in southern Australia (Keith et al., 2009). A global synthesis suggested that average AGB among high-biomass stands in wet temperate forests (~377 Mg C ha^{-1}) was over twice that of high-biomass stands in wet tropical forests (~179 Mg C ha^{-1}) and

nearly six times that of high-biomass stands in wet boreal forests (~64 Mg C ha^{-1}) (Keith et al., 2009). The range in BIO included in our analysis of WAORCA thus spanned much of the observed global range in BIO.

Both field and satellite measurements revealed that median BIO increased with $CMI_{\overline{wy}}$, yet the satellite data set showed less of an increase than the field measurements. Median forest BIO_{field} increased nearly 1,000% between the dry woodlands and coastal temperate rainforests in WAORCA, yet the increase in BIO_{sat} with increasing $CMI_{\overline{wy}}$ was less pronounced (~410% increase) when assessed across the western US. Furthermore, median BIO_{sat} plateaued around 175 Mg C ha^{-1} in areas where $CMI_{\overline{wy}}$ was ~100-200 cm yr^{-1}. The response of BIO to increasing $CMI_{\overline{wy}}$ was likely more muted when assessed using the satellite-derived maps than the field measurements for several reasons. The maps are largely derived from optical, multi-spectral satellite imagery that is not very sensitive to variation in BIO in high-biomass forests. Additionally, areas with high BIO often occur as small patches set in a matrix of stands with lower BIO (Spies et al., 1994) and thus the moderate-resolution satellite imagery used in developing these maps records the spectral signature of this larger area rather than just the patch with high BIO. In other words, the satellite imagery has a larger sampling footprint relative to that of a field plot, which thus averages BIO over a larger area, reducing peak values. Advances in satellite remote sensing, such as NASA's new Global Ecosystem Dynamics Investigation Lidar (GEDI) instrument, are anticipated to help overcome some of these challenges (Goetz and Dubayah, 2011). Nevertheless, current BIO maps (e.g., Kellndorfer et al., 2012; Wilson et al., 2013) proved a valuable tool for ecologic and natural resource assessments (Berner et al., 2012; Goetz et al., 2014; Krankina et al., 2014).

426

427 ### 4.4 Carbon residence time in tree biomass

428 We computed CRT as BIO/NPP and found that median CRT_{field} increased persistently with
429 $CMI_{\overline{wy}}$ from ~11 years in the driest forests to over 49 years in the wettest forests, highlighting a
430 fundamental change in ecosystem function along this broad bioclimatic gradient. One limitation
431 of our study is that computing CRT in this manner assumes that BIO is constant over time
432 (Friend et al., 2014). We focused on mature stands (>100 years) to minimize the change in BIO
433 over time, though acknowledge that BIO can gradually increase during subsequent centuries
434 (Hudiburg et al., 2009), which would lead us to underestimated CRT. Conversely, drought and
435 insect-induced defoliation in the early 2000s could have suppressed NPP (Schwalm et al., 2012;
436 Berner and Law, 2015) without a proportional reduction in BIO, which could have inflated our
437 estimates of CRT in some areas. Nevertheless, our results agree well with a prior study focused
438 on 11 LTERS spread across the conterminous US that found CRT increased from ~2 years in a
439 desert shrubland to ~73 years in 450-years old Douglas-fir stand at the Andrews LTER in the
440 Oregon Cascade Mountains (Webb et al., 1983). For comparison, we looked at five old-growth
441 Douglas-fir stands (336-555 years old) near the Andrews LTER and found that CRT_{field} averaged
442 79±23 years (± 1SD) among these stands. An increase in the CRT of aboveground tissues was
443 also observed among plant communities along an elevational moisture gradient in the Santa
444 Catalina Mountains of Arizona (Whittaker and Niering, 1975) and across nine mature stands in a
445 range of forest communities in Oregon (Gholz, 1982). Although this pattern has been previously
446 documented at small scales, the underlying mechanisms remain unclear.

We speculate that the increase in CRT with increased water availability was associated with underlying changes in NPP allocation, BIO mortality rates, and stand age. Trees invest a larger proportion of NPP into aboveground tissue production as conditions become wetter and competition for light intensifies (Runyon et al., 1994; Law et al., 2003). Our field measurements suggested that the fraction of NPP allocated aboveground increased from ~0.45 in the driest areas to ~0.64 in the wettest areas and, furthermore, that CRT in aboveground tissues averaged twice as long as CRT in belowground tissues. Thus, a shift in NPP allocation toward longer-lived aboveground tissues likely contributed to longer CRT in wetter areas. Longer CRT in wetter areas could also be related to forests in these areas (e.g., Coast Range) experiencing lower BIO mortality rates from wildfire and bark beetles than forests in drier, continental areas (Hicke et al., 2013). We also found that mature stands tended to be older in wetter areas and that older stands tended to have longer CRT, likely as a result of these stands having higher BIO and similar NPP (Hudiburg et al., 2009). Consequently, the CRT-$CMI_{\overline{wy}}$ relationships that we observed incorporate an age-related effect; however, the effect was quite small relative to the climate-effect. This can be illustrated by comparing median CRT between mature (100-200 years) and old (>200 years) stands occupying very dry ($CMI_{\overline{wy}}$< -100 cm yr^{-1}) and very wet ($CMI_{\overline{wy}}$ > 100 cm yr^{-1}) areas. Median CRT differed by 6% (16 vs. 17 years) between mature and old stands in very dry areas and by 10% (47 vs. 52 years) in very wet areas. Conversely, median CRT of mature stands differed 98% (16 vs. 47 years) between very dry and very wet areas, while the median CRT of old stands differed 101% (52 vs. 17 years) between very dry and very wet areas. In other words, the difference in CRT between stands in contrasting climates is much greater than difference in CRT between mature and old stands within a climate zone. Our study demonstrates that CRT in live tree biomass was strongly influenced by water availability, yet

additional efforts are needed to determine the underlying mechanism by which changes in water availability affect CRT, particularly given that CRT is a primary source of uncertainty in global vegetation model projections of future terrestrial carbon cycling (Friend et al., 2014).

4.5 Predicting ecosystem response to environmental change

Water availability is projected to decline in much of the western US over the coming century, in part due to higher temperatures increasing atmospheric evaporative demand (Dai, 2013; Walsh et al., 2014; Cook et al., 2015). Predicting the timing, magnitude and extent of ecological response to regional climate change remains a challenge. Our study showed that water availability is a key determinant of forest structure and function in the western US, broadly suggesting that chronic reductions in regional water availability could reduce the NPP, BIO, and CRT in mature stands. Nevertheless, it is problematic to predict the temporal response of extant forest communities to near-term climatic change based on bioclimatic relationships derived from spatial data. For instance, recent studies found that the slope of the NPP-precipitation relationship was much steeper when derived from spatial data than when derived from the temporal response of NPP to interannual variation in precipitation (Jin and Goulden, 2014; Wilcox et al., 2016). Near-term effects of climate variability depend on the physiological characteristics of species in the extant plant community, yet bioclimatic relationships derived from spatial data reflect gradual adjustment of community composition and population size to climate over long periods of time (Jin and Goulden, 2014; Wilcox et al., 2016). Furthermore, bioclimatic models derived from spatial data cannot account for other ecophysiological impacts of environmental change, such as (1) enhanced plant water use efficiency from CO_2 fertilization (Soulé and Knapp, 2015); (2)

492 increased likelihood of tree mortality due to hotter drought (Adams et al., 2009); or (3) novel
493 changes in disturbance regimes (Dale et al., 2001; Hicke et al., 2006). Consequently, predicting
494 ecological response to environmental change over the coming century will require the use of
495 mechanistic ecosystem models that account for physiologic, demographic, and disturbance
496 processes at fine taxonomic and spatial scales (Hudiburg et al., 2013; Law, 2014). Although
497 spatial models may not be suitable for near-term projection of ecosystems change, they do
498 provide insight into long-term ecosystem adaptation to local climate and, furthermore, can be
499 used to validate and refine mechanistic models if constructed from a representative sample of
500 forestlands.

501

502 **4.6 Summary and conclusions**

503 Water availability varies widely across the western US, giving rise to forests that range from dry,
504 low-biomass woodlands to temperate rainforests that are among highest biomass forests found
505 anywhere in the world. In this study we quantified changes in tree productivity, live biomass, and
506 carbon residence time along spatial gradients in water availability using field inventory
507 measurements from WAORCA and satellite remote sensing data sets spanning the western US.
508 Our multi-method, multi-scale analysis revealed that tree productivity, live biomass, and carbon
509 residence time all increased notably with water availability, which we computed using an index
510 that accounted for both precipitation and reference evapotranspiration. The observed increase in
511 productivity was likely due to the close coupling between carbon and water cycling at leaf to
512 ecosystem scales, while the observed increase in live biomass was associated with higher
513 productivity and longer carbon residence. The increase in carbon residence time in wetter areas

514 was linked with greater carbon allocation to long-lived aboveground tissues, older stand age,
515 and, possibly, lower biomass mortality rates from natural disturbance (e.g., bark beetles, fires).
516 Tree productivity and biomass derived from field- and satellite-measurements exhibited similar
517 responses to increasing water availability, though the satellite data sets tended to plateau in the
518 wettest areas, suggesting that additional efforts are needed to better quantify productivity and
519 biomass from satellites in high-productivity, high-biomass forests. The pronounced increase in
520 tree productivity, biomass, and carbon residence time between the driest and wettest areas
521 illustrates the gradual adjustment of ecosystem structure and function to long-term variation in
522 water availability; however, the observed bioclimatic relationships are not suitable for near-term
523 projections of future ecosystem response to regional drying. Predicting near-term ecosystem
524 response to drying and other environmental change (e.g., increased CO_2) will require
525 mechanistic ecosystem models, which can be evaluated against bioclimatic relationships
526 developed using inventory sites from a representative sample of forestlands (e.g., Forest Service
527 inventory sites). Overall, our results indicate that water availability is a key determinant of tree
528 productivity, live biomass, and carbon residence time in mature stands ranging from dry
529 woodlands to coastal temperate rainforests. Future efforts are needed to anticipate and mitigate
530 the impacts of projected warming and drying on forest ecosystems in the western US and
531 elsewhere around the world.

532

533 **Author contributions**

534 L.T.B. designed the study, analyzed the data, and prepared the manuscript with contributions
535 from B.E.L. and T.W.H., who both also contributed data sets to this effort.

536

537 **Data Availability**

538 The data sets that we used in this analysis are nearly all publicly available online. In particular
539 MODIS NPP are available from the Numerical Terradynamic Simulation Group at the University
540 of Montana and MODIS LAI can be accessed using the NASA Reverb data portal. The satellite-
541 derived biomass data sets are available from the Oak Ridge National Laboratory Distributed
542 Active Archive Center for Biogeochemical Dynamics and the US Forest Service. The forest
543 inventory data can be attained from the USFS Forest Inventory and Analysis program, while the
544 derived estimates of forest biomass and productivity are available on request.

545

546 **Acknowledgements**

547 This work was supported by NASA Headquarters under the NASA Earth and Space Science
548 Fellowship Program (Grant NNX14AN65H), the USDA National Institute of Food and
549 Agriculture (Grant 2013-67003-20652), and the ARCS Foundation Scholar program. T.W.H.
550 was supported by the National Science Foundation Idaho EPSCoR Program (Grant IIA-
551 1W301792). We thank Charles Bourque for serving as the handling associate editor for our
552 manuscript and also thank four anonymous reviewers for their constructive feedback. We cite no
553 conflicts of interest.

554

555 **References**

556 Adams, H. D., Guardiola-Claramonte, M., Barron-Gafford, G. A., Villegas, J. C., Breshears, D. D., Zou, C. B.,
557 Troch, P. A., and Huxman, T. E.: Temperature sensitivity of drought-induced tree mortality portends
558 increased regional die-off under global-change-type drought, Proceedings of the National Academy of
559 Sciences of the United States of America, 106, 7063-7066, 10.1073/pnas.0901438106, 2009.
560 Allen, R. G., Pereira, L. S., Raes, D., and Smith, M.: Crop evapotranspiration-Guidelines for computing
561 crop water requirements-FAO Irrigation and drainage paper 56, FAO, Rome, 300, 1998.
562 Ball, J. T., Woodrow, I. E., and Berry, J. A.: A model predicting stomatal conductance and its contribution
563 to the control of photosynthesis under different environmental conditions, in: Progress in
564 photosynthesis research, Springer, 221-224, 1987.
565 Bechtold, W., and Patterson, P.: The enhanced forest inventory and analysis program-- national
566 sampling design and estimation procedures, USDA Forest Service General Technical Report SRS-80,
567 Asheville, NC, 98, 2005.
568 Berner, L. T., Beck, P. S. A., Loranty, M. M., Alexander, H. D., Mack, M. C., and Goetz, S. J.: Cajander larch
569 (Larix cajanderi) biomass distribution, fire regime and post-fire recovery in northeastern Siberia,
570 Biogeosciences, 9, 3943-3959, 10.5194/bg-9-3943-2012, 2012.
571 Berner, L. T., Beck, P. S. A., Bunn, A. G., and Goetz, S. J.: Plant response to climate change along the
572 forest-tundra ecotone in northeastern Siberia, Global Change Biology, 19, 3449-3462,
573 10.1111/gcb.12304, 2013.
574 Berner, L. T., and Law, B. E.: Water limitations on forest carbon cycling and conifer traits along a steep
575 climatic gradient in the Cascade Mountains, Oregon, Biogeosciences, 12, 6617-6635, 2015.
576 Berner, L. T., and Law, B. E.: Plant traits, productivity, biomass and soil properties from forest sites in the
577 Pacific Northwest, 1999–2014, Scientific Data, 3, 160002, 10.1038/sdata.2016.2, 2016.
578 Blackard, J., Finco, M., Helmer, E., Holden, G., Hoppus, M., Jacobs, D., Lister, A., Moisen, G., Nelson, M.,
579 and Riemann, R.: Mapping US forest biomass using nationwide forest inventory data and moderate
580 resolution information, Remote Sensing of Environment, 112, 1658-1677, 2008.
581 Cairns, M. A., Brown, S., Helmer, E. H., and Baumgardner, G. A.: Root biomass allocation in the world's
582 upland forests, Oecologia, 111, 1-11, 1997.
583 Carroll, A. L., Sillett, S. C., and Kramer, R. D.: Millennium-Scale Crossdating and Inter-Annual Climate
584 Sensitivities of Standing California Redwoods, PLoS ONE, 9, e102545, 10.1371/journal.pone.0102545,
585 2014.
586 Churkina, G., and Running, S. W.: Contrasting climatic controls on the estimated productivity of global
587 terrestrial biomes, Ecosystems, 1, 206-215, 1998.
588 Collins, M., Knutti, R., Arblaster, J., Dufresne, J.-L., Fichefet, T., Friedlingstein, P., Gao, X., Gutowski, W. J.,
589 Johns, T., Krinner, G., Shongwe, M., Tebaldi, C., Weaver, A. J., and Wehner, M.: Long-term Climate
590 Change: Projections, Commitments and Irreversibility, in: Climate Change 2013: The Physical Science
591 Basis. Contribution of Working Group I to the Fifth Assessment Report of the Intergovernmental Panel
592 on Climate Change, edited by: Stocker, T. F., Qin, D., Plattner, G.-K., Tignor, M., Allen, S. K., Boschung, J.,
593 Nauels, A., Xia, Y., Bex, V., and Midgley, P. M., Cambridge University Press, Cambridge, United Kingdom
594 and New York, NY, USA, 1029–1136, 2013.
595 Cook, B. I., Ault, T. R., and Smerdon, J. E.: Unprecedented 21st century drought risk in the American
596 Southwest and Central Plains, Science Advances, 1, e1400082, 2015.
597 Dai, A.: Increasing drought under global warming in observations and models, Nature Climate Change, 3,
598 52-58, doi: 10.1038/nclimate1633, 2013.
599 Dale, V. H., Joyce, L. A., McNulty, S., Neilson, R. P., Ayres, M. P., Flannigan, M. D., Hanson, P. J., Irland, L.
600 C., Lugo, A. E., Peterson, C. J., Simberloff, D., Swanson, F. J., Stocks, B. J., and Michael Wotton, B.:
601 Climate Change and Forest Disturbances, BioScience, 51, 723-734, 10.1641/0006-
602 3568(2001)051[0723:ccafd]2.0.co;2, 2001.

603 Daly, C., Halbleib, M., Smith, J. I., Gibson, W. P., Doggett, M. K., Taylor, G. H., Curtis, J., and Pasteris, P. P.:
604 Physiographically sensitive mapping of climatological temperature and precipitation across the
605 conterminous United States, International Journal of Climatology, 28, 2031-2064, 2008.
606 Dawson, T. E.: Fog in the California redwood forest: ecosystem inputs and use by plants, Oecologia, 117,
607 476-485, 1998.
608 Droogers, P., and Allen, R. G.: Estimating reference evapotranspiration under inaccurate data conditions,
609 Irrigation and drainage systems, 16, 33-45, 2002.
610 Fischer, D. T., Still, C. J., Ebert, C. M., Baguskas, S. A., and Park Williams, A.: Fog drip maintains dry
611 season ecological function in a California coastal pine forest, Ecosphere, 7, 2016.
612 Friedl, M. A., Sulla-Menashe, D., Tan, B., Schneider, A., Ramankutty, N., Sibley, A., and Huang, X.: MODIS
613 Collection 5 global land cover: Algorithm refinements and characterization of new datasets, Remote
614 Sensing of Environment, 114, 168-182, 2010.
615 Friend, A. D., Lucht, W., Rademacher, T. T., Keribin, R., Betts, R., Cadule, P., Ciais, P., Clark, D. B.,
616 Dankers, R., and Falloon, P. D.: Carbon residence time dominates uncertainty in terrestrial vegetation
617 responses to future climate and atmospheric CO2, Proceedings of the National Academy of Sciences,
618 111, 3280-3285, 2014.
619 Gholz, H. L.: Environmental Limits on Aboveground Net Primary Production, Leaf Area, and Biomass in
620 Vegetation Zones of the Pacific Northwest, Ecology, 63, 469-481, 10.2307/1938964, 1982.
621 Girardin, C. A. J., Malhi, Y., Aragao, L., Mamani, M., Huaraca Huasco, W., Durand, L., Feeley, K., Rapp, J.,
622 SILVA-ESPEJO, J., and Silman, M.: Net primary productivity allocation and cycling of carbon along a
623 tropical forest elevational transect in the Peruvian Andes, Global Change Biology, 16, 3176-3192, 2010.
624 Goetz, S., and Dubayah, R.: Advances in remote sensing technology and implications for measuring and
625 monitoring forest carbon stocks and change, Carbon Management, 2, 231-244, 10.4155/cmt.11.18,
626 2011.
627 Goetz, S. J., Sun, M., Zolkos, S., Hansen, A., and Dubayah, R.: The relative importance of climate and
628 vegetation properties on patterns of North American breeding bird species richness, Environmental
629 Research Letters, 9, 034013, 2014.
630 Hargreaves, G. H., and Samani, Z. A.: Reference crop evapotranspiration from temperature, Applied
631 Engineering in Agriculture, 1, 96-99, 1985.
632 Hicke, J. A., Logan, J. A., Powell, J., and Ojima, D. S.: Changing temperatures influence suitability for
633 modeled mountain pine beetle (Dendroctonus ponderosae) outbreaks in the western United States,
634 Journal of Geophysical Research: Biogeosciences (2005–2012), 111, 2006.
635 Hicke, J. A., Meddens, A. J., Allen, C. D., and Kolden, C. A.: Carbon stocks of trees killed by bark beetles
636 and wildfire in the western United States, Environmental Research Letters, 8, 035032, 2013.
637 Hijmans, R. J., and van Etten, J.: raster: Geographic analysis and modeling with raster data, 2.1-25 ed., R
638 Foundation for Statistical Computing, Vienna, 2013.
639 Hogg, E., Brandt, J. P., and Kochtubajda, B.: Growth and dieback of aspen forests in northwestern
640 Alberta, Canada, in relation to climate and insects, Canadian Journal of Forest Research, 32, 823-832,
641 2002.
642 Hogg, E., Brandt, J., and Michaelian, M.: Impacts of a regional drought on the productivity, dieback, and
643 biomass of western Canadian aspen forests, Canadian Journal of Forest Research, 38, 1373-1384, 2008.
644 Hogg, E. H.: Climate and the southern limit of the western Canadian boreal forest, Canadian Journal of
645 Forest Research, 24, 1835-1845, 1994.
646 Hogg, E. H., and Hurdle, P.: The aspen parkland in western Canada: A dry-climate analogue for the future
647 boreal forest?, Water, Air, and Soil Pollution, 82, 391-400, 1995.
648 Holdridge, L. R.: Determination of World Plant Formations From Simple Climatic Data, Science, 105, 367-
649 368, 10.1126/science.105.2727.367, 1947.

650 Hudiburg, T., Law, B., Turner, D. P., Campbell, J., Donato, D., and Duane, M.: Carbon dynamics of Oregon
651 and Northern California forests and potential land-based carbon storage, Ecological Applications, 19,
652 163-180, 2009.
653 Hudiburg, T. W., Law, B. E., Wirth, C., and Luyssaert, S.: Regional carbon dioxide implications of forest
654 bioenergy production, Nature Climate Change, 1, 419-423, 10.1038/nclimate1264, 2011.
655 Hudiburg, T. W., Law, B. E., and Thornton, P. E.: Evaluation and improvement of the Community Land
656 Model (CLM4) in Oregon forests, Biogeosciences, 10, 453-470, 10.5194/bg-10-453-2013, 2013.
657 Jin, Y., and Goulden, M. L.: Ecological consequences of variation in precipitation: separating short-versus
658 long-term effects using satellite data, Global Ecology and Biogeography, 23, 358-370, 2014.
659 Johnstone, J. A., and Dawson, T. E.: Climatic context and ecological implications of summer fog decline in
660 the coast redwood region, Proceedings of the National Academy of Sciences, 107, 4533-4538, 2010.
661 Keith, H., Mackey, B. G., and Lindenmayer, D. B.: Re-evaluation of forest biomass carbon stocks and
662 lessons from the world's most carbon-dense forests, Proceedings of the National Academy of Sciences,
663 106, 11635-11640, 2009.
664 Kellndorfer, J., Walker, W., LaPoint, E., Bishop, J., Cormier, T., Fiske, G., Hoppus, M., Kirsch, K., and
665 Westfall, J.: NACP Aboveground Biomass and Carbon Baseline Data (NBCD 2000), U.S.A., 2000 Data set,
666 ORNL DAAC, Oak Ridge, Tennessee, U.S.A. , 2012.
667 Krankina, O. N., DellaSala, D. A., Leonard, J., and Yatskov, M.: High-Biomass Forests of the Pacific
668 Northwest: Who Manages Them and How Much is Protected?, Environmental Management, 54, 112-
669 121, 2014.
670 Law, B. E., Thornton, P. E., Irvine, J., Anthoni, P. M., and Van Tuyl, S.: Carbon storage and fluxes in
671 ponderosa pine forests at different developmental stages, Global Change Biology, 7, 755-777, 2001.
672 Law, B. E., Falge, E., Gu, L. V., Baldocchi, D. D., Bakwin, P., Berbigier, P., Davis, K., Dolman, A. J., Falk, M.,
673 and Fuentes, J. D.: Environmental controls over carbon dioxide and water vapor exchange of terrestrial
674 vegetation, Agricultural and Forest Meteorology, 113, 97-120, 2002.
675 Law, B. E., Sun, O. J., Campbell, J., Van Tuyl, S., and Thornton, P. E.: Changes in carbon storage and fluxes
676 in a chronosequence of ponderosa pine, Global Change Biology, 9, 510-524, 2003.
677 Law, B. E.: Regional analysis of drought and heat impacts on forests: current and future science
678 directions, Global Change Biology, 20, 3595-3599, 10.1111/gcb.12651, 2014.
679 Major, J.: A climatic index to vascular plant activity, Ecology, 44, 485-498, 1963.
680 Means, J. E., Hansen, H. A., Koerper, G. J., Alaback, P. B., and Klopsch, M. W.: Software for computing
681 plant biomass--BIOPAK users guide, U.S. Department of Agriculture, Forest Service, Pacific Northwest
682 Research Station, Portland, OR, 184, 1994.
683 Mitchell, K. E., Lohmann, D., Houser, P. R., Wood, E. F., Schaake, J. C., Robock, A., Cosgrove, B. A.,
684 Sheffield, J., Duan, Q., and Luo, L.: The multi-institution North American Land Data Assimilation System
685 (NLDAS): Utilizing multiple GCIP products and partners in a continental distributed hydrological
686 modeling system, Journal of Geophysical Research: Atmospheres, 109, 2004.
687 Myneni, R., Hoffman, S., Knyazikhin, Y., Privette, J., Glassy, J., Tian, Y., Wang, Y., Song, X., Zhang, Y., and
688 Smith, G.: Global products of vegetation leaf area and fraction absorbed PAR from year one of MODIS
689 data, Remote sensing of environment, 83, 214-231, 2002.
690 Nakawatase, J. M., and Peterson, D. L.: Spatial variability in forest growth-climate relationships in the
691 Olympic Mountains, Washington, Canadian journal of forest research, 36, 77-91, 2006.
692 Neeti, N., and Kennedy, R.: Comparison of national level biomass maps for conterminous US:
693 understanding pattern and causes of differences, Carbon Balance and Management, 11, 19,
694 10.1186/s13021-016-0060-y, 2016.
695 Olson, J. S.: Energy storage and the balance of producers and decomposers in ecological systems,
696 Ecology, 44, 322-331, 1963.

697 Pan, Y., Chen, J. M., Birdsey, R., McCullough, K., He, L., and Deng, F.: Age structure and disturbance
698 legacy of North American forests, 2011.
699 Peterman, W., Waring, R. H., Seager, T., and Pollock, W. L.: Soil properties affect pinyon pine–juniper
700 response to drought, Ecohydrology, 6, 455-463, 2013.
701 R Core Team: R: A Language and Environment for Statistical Computing, R Foundation for Statistical
702 Computing, Vienna, 2015.
703 Ruefenacht, B., Finco, M., Nelson, M., Czaplewski, R., Helmer, E., Blackard, J., Holden, G., Lister, A.,
704 Salajanu, D., and Weyermann, D.: Conterminous US and Alaska forest type mapping using forest
705 inventory and analysis data, Photogramm. Eng. Remote Sens, 74, 1379-1388, 2008.
706 Ruehr, N., Law, B., Quandt, D., and Williams, M.: Effects of heat and drought on carbon and water
707 dynamics in a regenerating semi-arid pine forest: a combined experimental and modeling approach,
708 Biogeosciences, 11, 4139-4156, 2014.
709 Running, S. W.: Testing Forest-BGC Ecosystem Process Simulations Across a Climatic Gradient in Oregon,
710 Ecological Applications, 4, 238-247, 1994.
711 Running, S. W., Nemani, R. R., Heinsch, F. A., Zhao, M., Reeves, M., and Hashimoto, H.: A continuous
712 satellite-derived measure of global terrestrial primary production, BioScience, 54, 547-560, 2004.
713 Runyon, J., Waring, R., Goward, S., and Welles, J.: Environmental limits on net primary production and
714 light-use efficiency across the Oregon transect, Ecological Applications, 4, 226-237, 1994.
715 Sanford, W. E., and Selnick, D. L.: Estimation of Evapotranspiration Across the Conterminous United
716 States Using a Regression With Climate and Land-Cover Data1, JAWRA Journal of the American Water
717 Resources Association, 49, 217-230, 2013.
718 Schroeder, P. E., McCandlish, B., Waring, R. H., and Perry, D. A.: The relationship of maximum canopy
719 leaf area to forest growth in eastern Washington, Northwest Science, 56, 121-130, 1982.
720 Schuur, E. A.: Productivity and global climate revisited: the sensitivity of tropical forest growth to
721 precipitation, Ecology, 84, 1165-1170, 2003.
722 Schwalm, C. R., Williams, C. A., Schaefer, K., Baldocchi, D., Black, T. A., Goldstein, A. H., Law, B. E.,
723 Oechel, W. C., and Scott, R. L.: Reduction in carbon uptake during turn of the century drought in western
724 North America, Nature Geoscience, 5, 551-556, 2012.
725 Smith, J. E., Heath, L. S., Skog, K. E., and Birdsey, R. A.: Methods for calculating forest ecosystem and
726 harvested carbon with standard estimates for forest types of the United States, USDA Forest Service
727 General Technical Report NE-343, Newtown Square, PA, 222, 2006.
728 Soulé, P. T., and Knapp, P. A.: Analyses of intrinsic water-use efficiency indicate performance differences
729 of ponderosa pine and Douglas-fir in response to CO2 enrichment, Journal of Biogeography, 42, 144-
730 155, 2015.
731 Spies, T. A., Ripple, W. J., and Bradshaw, G.: Dynamics and pattern of a managed coniferous forest
732 landscape in Oregon, Ecological Applications, 4, 555-568, 1994.
733 Thomas, C. K., Law, B. E., Irvine, J., Martin, J. G., Pettijohn, J. C., and Davis, K. J.: Seasonal hydrology
734 explains interannual and seasonal variation in carbon and water exchange in a semiarid mature
735 ponderosa pine forest in central Oregon, Journal of Geophysical Research: Biogeosciences (2005–2012),
736 114, 2009.
737 Van Tuyl, S., Law, B., Turner, D., and Gitelman, A.: Variability in net primary production and carbon
738 storage in biomass across Oregon forests—an assessment integrating data from forest inventories,
739 intensive sites, and remote sensing, Forest Ecology and Management, 209, 273-291, 2005.
740 Walsh, J., Wuebbles, D., Hayhoe, K., Kossin, J., Kunkel, K., Stephens, G., Thorne, P., Vose, R., Wehner, M.,
741 Willis, J., Anderson, D., Doney, S., Feely, R., Hennon, P., Kharin, V., Knutson, T., Landerer, F., Lenton, T.,
742 Kennedy, J., and Somerville, R.: Our Changing Climate, in: Climate Change Impacts in the United States:

The Third National Climate Assessment, edited by: Melillo, J. M., Richmond, T. C., and Yohe, G. W., U.S. Global Change Research Program, 19-67, 2014.
Waring, R.: Estimating forest growth and efficiency in relation to canopy leaf area, Adv. Ecol. Res, 13, 327-354, 1983.
Waring, R. H., and Franklin, J. F.: Evergreen coniferous forests of the Pacific Northwest, Science, 204, 1380-1386, 1979.
Waring, R. H., and Running, S. W.: Forest Ecosystems: Analysis at Multiple Scales, 3rd ed., Elsevier Academic Press, Burlington, MA, 420 pp., 2007.
Webb, W. L., Lauenroth, W. K., Szarek, S. R., and Kinerson, R. S.: Primary production and abiotic controls in forests, grasslands, and desert ecosystems in the United States, Ecology, 134-151, 1983.
Whittaker, R. H.: Estimation of net primary production of forest and shrub communities, Ecology, 42, 177-180, 1961.
Whittaker, R. H., and Niering, W. A.: Vegetation of the Santa Catalina Mountains, Arizona. V. Biomass, production, and diversity along the elevation gradient, Ecology, 56, 771-790, 1975.
Wickham, H., and Francois, R.: dplyr: A Grammar of Data Manipulation, R package version 0.4.2, http://CRAN.R-project.org/package=dplyr, 2015.
Wilcox, K. R., Blair, J. M., Smith, M. D., and Knapp, A. K.: Does ecosystem sensitivity to precipitation at the site-level conform to regional-scale predictions?, Ecology, 97, 561-568, 2016.
Williams, A. P., Seager, R., Macalady, A. K., Berkelhammer, M., Crimmins, M. A., Swetnam, T. W., Trugman, A. T., Buenning, N., Noone, D., and McDowell, N. G.: Correlations between components of the water balance and burned area reveal new insights for predicting forest fire area in the southwest United States, International Journal of Wildland Fire, 24, 14-26, 10.1071/WF14023, 2014.
Williams, M., Rastetter, E., Fernandes, D., Goulden, M., Wofsy, S., Shaver, G., Melillo, J., Munger, J., Fan, S. M., and Nadelhoffer, K.: Modelling the soil-plant-atmosphere continuum in a Quercus–Acer stand at Harvard Forest: the regulation of stomatal conductance by light, nitrogen and soil/plant hydraulic properties, Plant, Cell & Environment, 19, 911-927, 1996.
Williams, M.: Deforesting the Earth: From Prehistory to Global Crisis, University of Chicago Press, Chicago, USA, 543 pp., 2006.
Wilson, B. T., Woodall, C., and Griffith, D.: Imputing forest carbon stock estimates from inventory plots to a nationally continuous coverage, Carbon balance and management, 8, 1, 2013.
Yan, K., Park, T., Yan, G., Liu, Z., Yang, B., Chen, C., Nemani, R. R., Knyazikhin, Y., and Myneni, R. B.: Evaluation of MODIS LAI/FPAR Product Collection 6. Part 2: Validation and Intercomparison, Remote Sensing, 8, 460, 2016.
Yang, Y., Fang, J., Ma, W., and Wang, W.: Relationship between variability in aboveground net primary production and precipitation in global grasslands, Geophysical Research Letters, 35, 2008.
Zhao, M., Running, S., Heinsch, F. A., and Nemani, R.: MODIS-derived terrestrial primary production, in: Land Remote Sensing and Global Environmental Change: NASA's Earth Observing System and the Science of ASTER and MODIS, edited by: Ramachandra, B., Justice, C. O., and Abrams, M. J., Springer, New York, 635-660, 2010.
Zotarelli, L., Dukes, M. D., Romero, C. C., Migliaccio, K. W., and Morgan, K. T.: Step by step calculation of the Penman-Monteith Evapotranspiration (FAO-56 Method), Institute of Food and Agricultural Sciences. University of Florida, 2010.

Tables

Table 1. Summary of tree net primary productivity (NPP; Mg C ha^{-1} yr^{-1}), live biomass (BIO; Mg C ha^{-1}), and carbon residence time (CRT; year) for stands over 100 years old across both WAORCA and the broader western US. These forest characteristics were quantified for WAORCA using field measurements from 1,953 sites and for the western US using satellite-derived data sets covering 18 Mha of mature forest. Satellite data sets included MODIS NPP and an estimate of BIO derived by combining existing maps of aboveground biomass with additional estimates of carbon storage in coarse root, fine roots, and foliage. These carbon stocks and fluxes combine above- and below-ground components.

Domain	Variable	Units	Time span	Mean (SD)	Range
WAORCA	NPP_{field}	Mg C ha^{-1} yr^{-1}	2001-2006	4.3 (2.5)	0.6 – 20.9
	BIO_{field}	Mg C ha^{-1}	2001-2006	158 (135)	2 – 947
	CRT_{field}	year	2001-2006	33 (19)	2 – 137
Western US	NPP_{sat}	Mg C ha^{-1} yr^{-1}	2000-2014	5.3 (2.0)	0.1 – 227
	BIO_{sat}	Mg C ha^{-1}	2000-2008	83 (54)	2 – 669
	CRT_{sat}	year	2000-2008	15 (9)	2 – 1390

Table 2. Changes in tree net primary productivity (NPP; Mg C ha^{-1} yr^{-1}), live biomass (BIO; Mg C ha^{-1}), and carbon residence time (CRT; year) for stands over 100 years old along gradients in a climate moisture index ($CMI_{\overline{wy}}$; cm yr^{-1}) in both WAORCA and the broader western US. Forest characteristics were quantified using field measurements in WAORCA and satellite remote sensing data sets covering the western US. The analysis incorporated forests in areas where $CMI_{\overline{wy}}$ was between -200 cm yr^{-1} and 200 cm yr^{-1}. Summaries include (1) median forest characteristic in the driest 5% and wettest 95% of sites/pixels; (2) the corresponding change; (3) and Spearman's correlation (r_s) between $CMI_{\overline{wy}}$ and the median forest characteristic computed at 10 cm yr^{-1} $CMI_{\overline{wy}}$ intervals. All correlations were statistically significant at $\alpha < 0.001$.

Domain	Variable	Units	Median of…		Change…		$CMI_{\overline{wy}}$ cor.
			Driest 5%	Wettest 95%	Abs.	%	r_s
WAORCA	NPP_{field}	Mg C ha^{-1} yr^{-1}	2.2	5.6	3.4	155	0.93
	BIO_{field}	Mg C ha^{-1}	26	281	255	997	0.96
	CRT_{field}	year	11	49	38	358	0.96
Western US	NPP_{sat}	Mg C ha^{-1} yr^{-1}	3.4	6.7	3.3	97	0.93
	BIO_{sat}	Mg C ha^{-1}	32	165	133	410	0.97
	CRT_{sat}	year	10	26	16	160	0.99

828

829

830

831

832

833

834

835

836 **Figures**

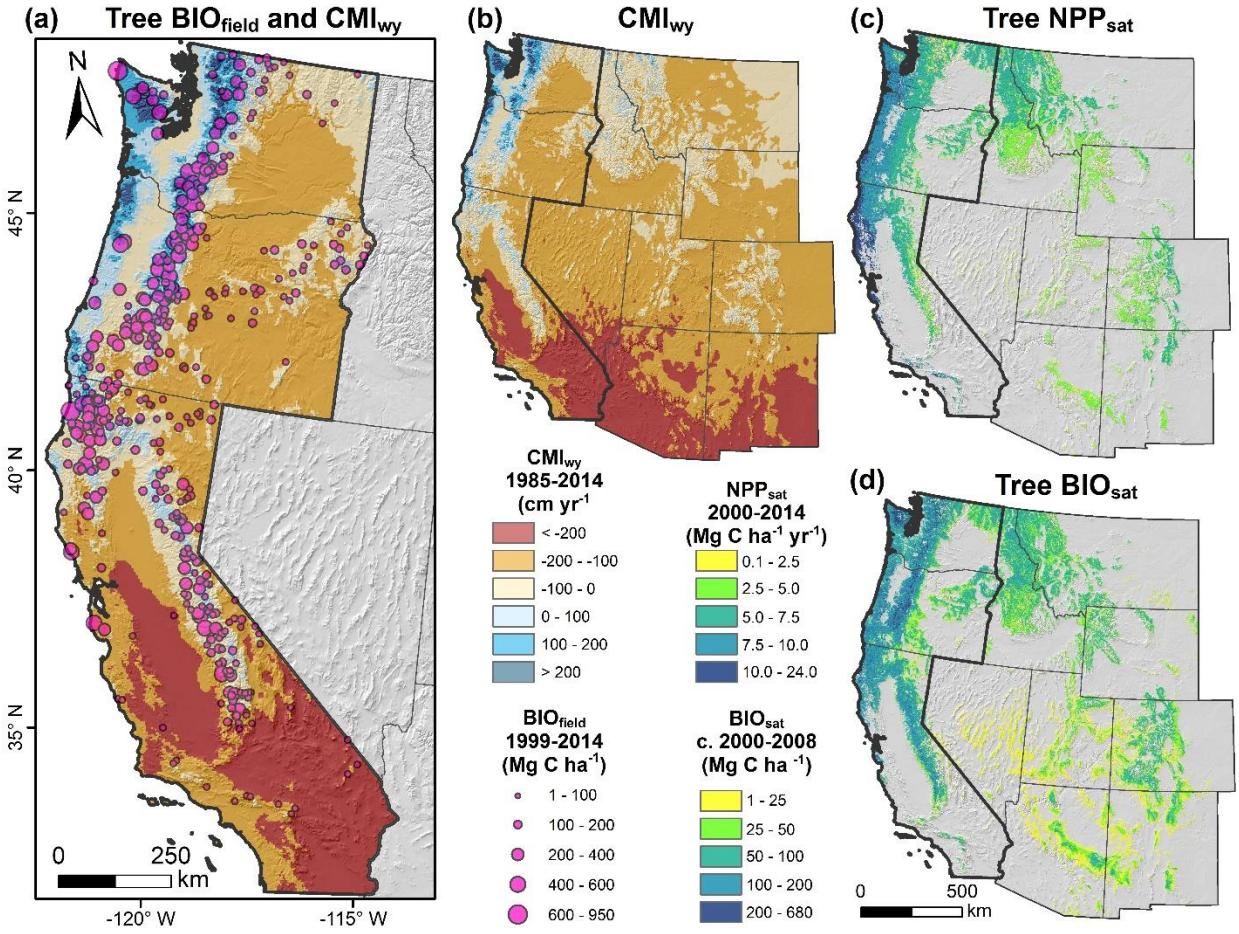

837

838 Figure 1. Mean climatic moisture index ($CMI_{\overline{wy}}$; cm yr^{-1}), tree net primary productivity (NPP;

839 Mg C ha^{-1} yr^{-1}), and live tree biomass (BIO; Mg C ha^{-1}) in the western US. (a) BIO derived from

840 field measurements (BIO_{field}) at mature sites (>100 years) in WAORCA. For visual clarity only
841 20% of the 1,953 sites are depicted. (b) The $CMI_{\overline{wy}}$ was computed as monthly precipitation
842 minus reference evapotranspiration summed over the annual water year (October-September)
843 and then averaged from 1985-2014. (c) Mean annual NPP was quantified using MODIS satellite
844 data from 2000-2014 (NPP_{sat}). (d) Tree BIO was quantified using satellite-derived estimates of
845 carbon stocks (BIO_{sat}).

846

847

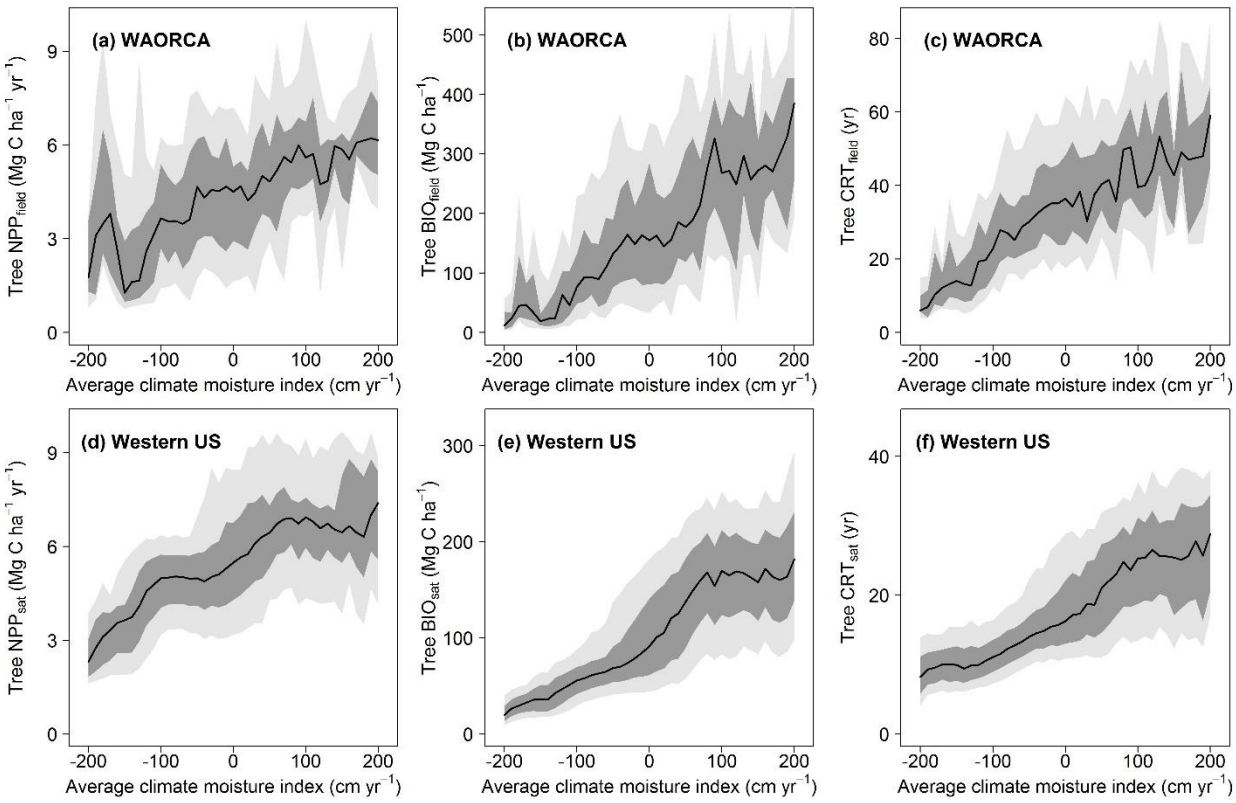

848

849 Figure 2. Tree net primary productivity (NPP; Mg C ha^{-1} yr^{-1}), live biomass (BIO; Mg C ha^{-1}),
850 and carbon residence time (CRT; years) increased with increasing water availability across both

851 WAORCA (a-c) and the broader western US (d-f). Forest characteristics were derived from field
852 measurements on 1,953 inventory plots in WAORCA (a-c) and from satellite remote sensing
853 data sets across 18 Mha of mature forest in the western US (d-f). NPP_{sat} was characterized using
854 MODIS data averaged annually from 2000 to 2014. BIO_{sat} was quantified based on an ensemble
855 of aboveground biomass maps plus estimates of coarse root, fine root, and foliage biomass. CRT
856 was computed for each field plot and pixel as BIO / NPP. Water availability was quantified using
857 a climate moisture index ($CMI= P-ET_0$) summed over the water year (October-September) and
858 then averaged from 1985-2014 ($\overline{CMI_{wy}}$). The region was partitioned into 10 cm yr^{-1} (non-
859 overlapping) $\overline{CMI_{wy}}$ bins, pixels/plots were allocated to bins, and then forest characteristics were
860 summarized within each bin. In each panel, the bold line denotes the median, dark gray band the
861 25-75th percentiles, and light gray band the 10-90th percentiles. Note the different y-axis scales
862 between (b) and (e), as well as (c) and (f).